Rössing Uranium Mine, Namibia: Insights into its Genesis from Structural Mapping and Ore Body Modeling

G. Greenway

Geology Department, Rössing Uranium Mine

I. J. Basson *

Department of Geological Sciences, University of Cape Town

(* Presenting)

Rössing

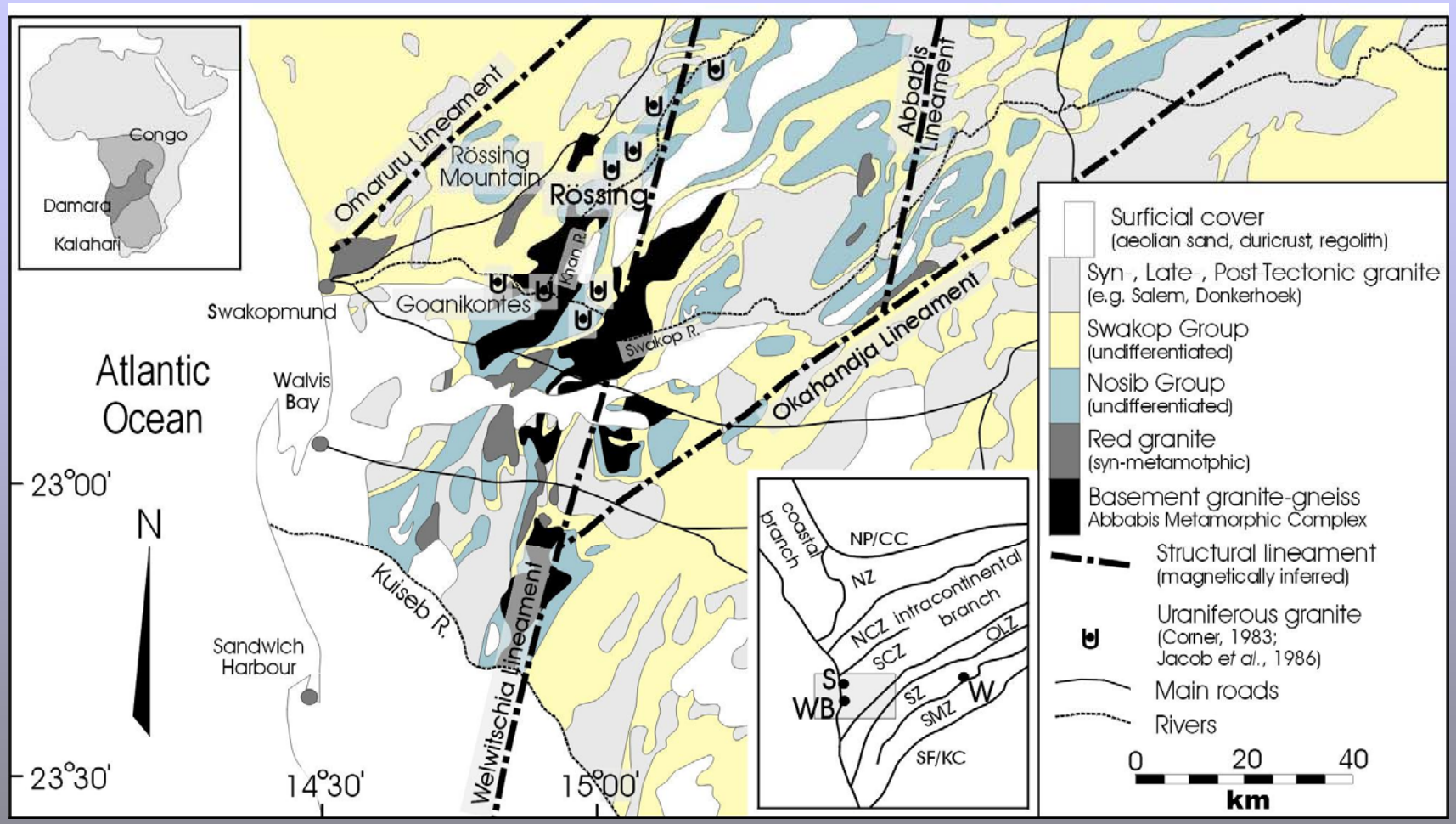

Modified after Smith (1965), Corner (1982, 1983) Miller (1983), Oliver (1995) and Eberle *et al.* (1995)

Rössing

Group & Nature	Formation	Member / Unit	Thickness (m)	Description
Swakop pelitic and calc.	Rössing	Metaquartzite	>100	Medium-grained quartzite, coarsening towards base
		Upper metapelitic gneiss	40-50	Diopside-biotite (-scapolite) gneiss; thin lenses of coarse-grained metaquartzite and marble; grading upwards into cordierite gneiss
		Upper marble	50-70	Serpentinitic and diopside-quartz-bearing marble; lenses of biotite-diopside granofels and cordierite-biotite gneiss
		Lower metapelitic gneiss	30-40	Cordierite-biotite-sillimanite gneiss; grading upwards into biotite-hornblende schist
		Lower marble	20-50	Dominant serpentinitic and minor graphitic marble; lenses of biotite-diopside granofels and pelitic schist
Nosib fluviatile	Khan	Amphibolite	10-20	Amphibole-biotite schist with relict pebble bands
		Upper gneiss	70-100	Amphibole- and pyroxene-gneiss
		Pyroxene-garnet Ortho-amphibolite gneiss	<120	Pyroxene-garnet gneiss and pods of hornblende-oligoclase ortho-amphibolite, often migmatized
		Lower gneiss	70-150	Strongly banded clinopyroxene-amphibole gneiss; migmatized in high-strain zones
	Etusis	Upper metaquartzite	>300 m	Arkosic and micaceous gneisses, feldspathic quartzites and biotite schist; extensively intruded by late- to post-kinematic granites and migmatized in high-strain zones
		Upper biotite schist		
		Lower metaquartzite		
		Lower biotite schist		
Abbabis Metamorphic Complex/Basement		-	-	Augen-, migmatitic-, biotite-, silimanite- and granite-gneiss; biotite schist and amphibolite

Lithostratgraphy of the Etusis, Khan and Rössing Formations in the vicinity of Rössing. The quoted thicknesses are approximate. Summarized after Nash (1971), SACS (1980), Coward (1983), Downing (1983), Martin (1983), Lehtonen *et al*. (1996) and Nex (1997). The glacio-marine Chuos Formation, which overlies the Rössing Formation, is not evident in the vicinity of Rössing and is not included.

Rössing

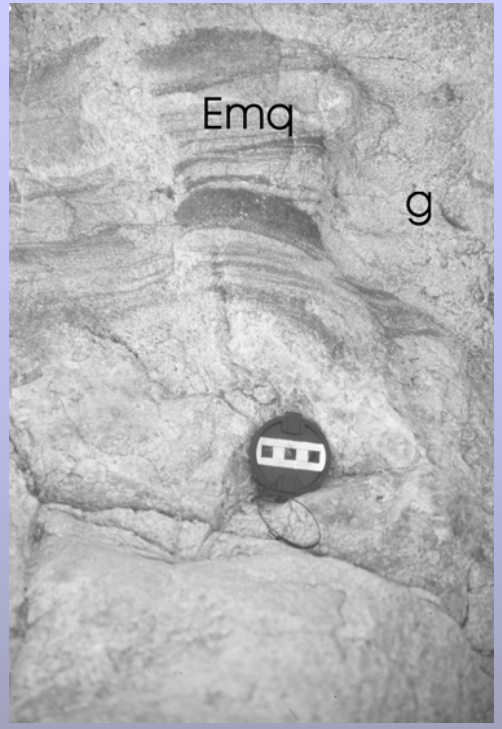

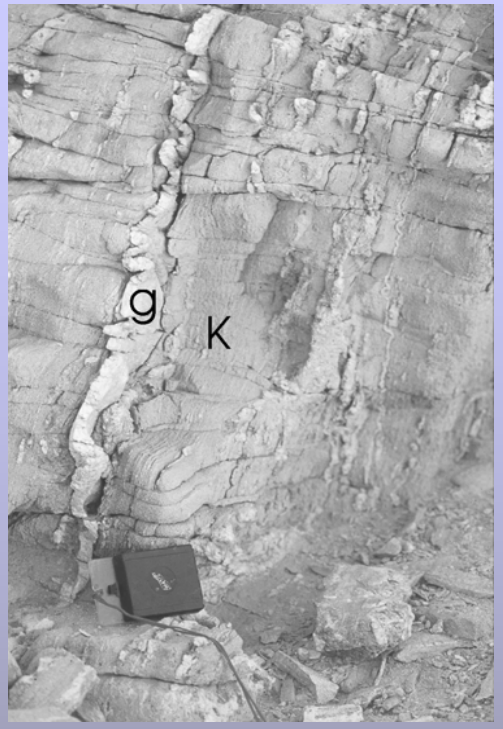

Examples of the main lithologies in the Rössing area

Rössing

Deformation Event	Major Fold Trend	Rössing Formation	Khan Formation	Etusis Formation
Original layering	-	Planar bedding in marbles and pyritic bands	Not evident in Rössing area	Relict heavy mineral layering in orthoquartzites
D_1	F_1 - Unknown	S_1 and S_2 laminar foliation in pelites	S_1 and S_2 migmatitic banding to the west of the Rössing Dome	S_1 and S_2 migmatitic banding
D_2	F_2 - NW (?)			
D_3	F_3 - NE	S_1 and S_2 transposed into sub-parallelism with S_3; flow folding in marbles	S_3 schistocity superimposed on migmatitic banding	Non-systematic brittle-ductile deformation of migmatitic banding
D_4	("F_4") NNE Rössing Dome Axis Orientation	Small, isolated folds with axial planar foliation (S_4)	Not discernible	Not discernible

Deformation events of the Rössing area, Central Zone, Damara Orogen, summarized from Smith (1965); Sawyer (1978), Martin (1983), Coward (1983) and Buhn and Stannistreet (1992/3). Note that the "F_4" folding trend is not due to a fold event (*sensu stricto*), but is rather a result of dome rotation.

Rössing

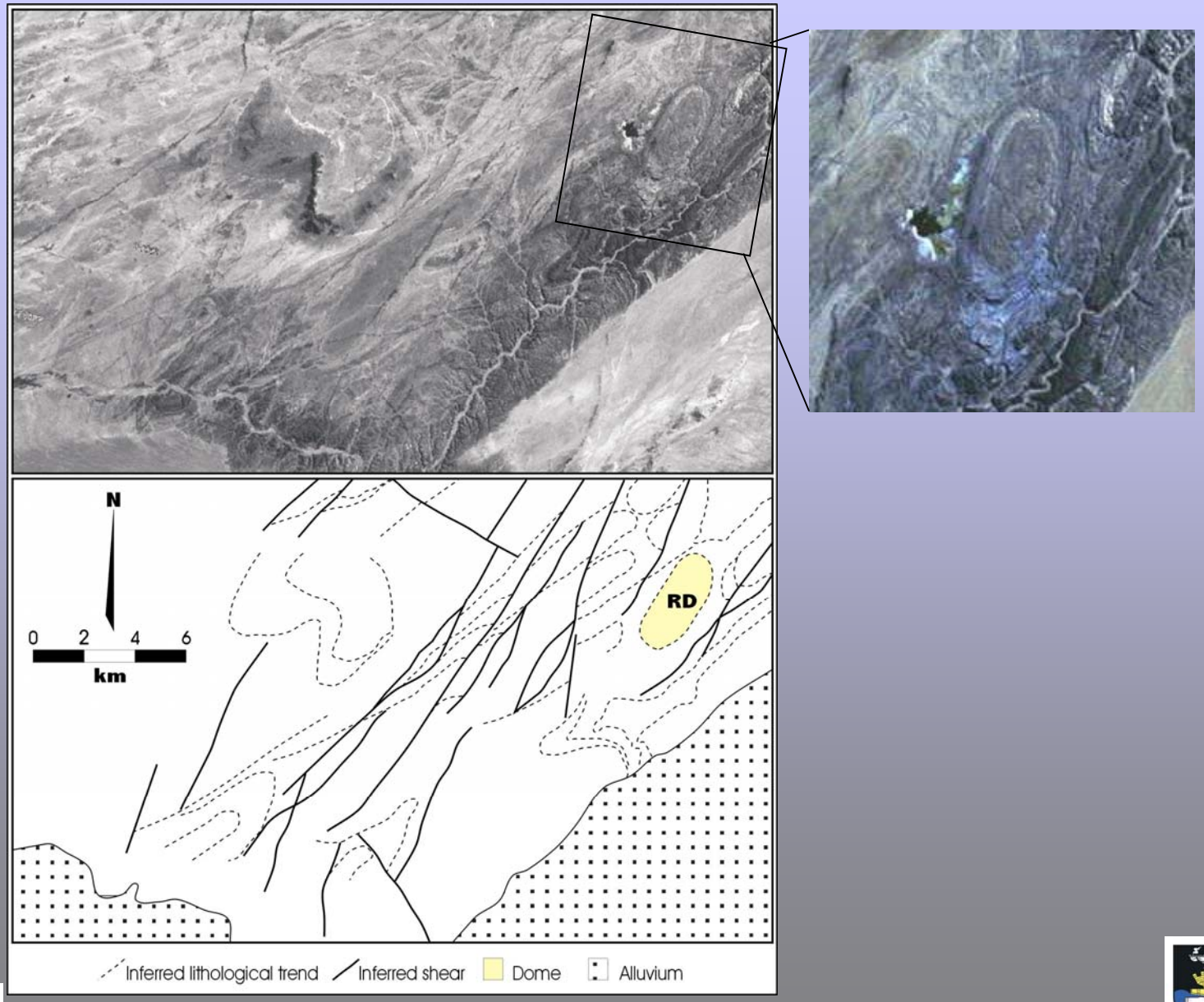

LandSat Courtesy of Rössing Uranium Mine

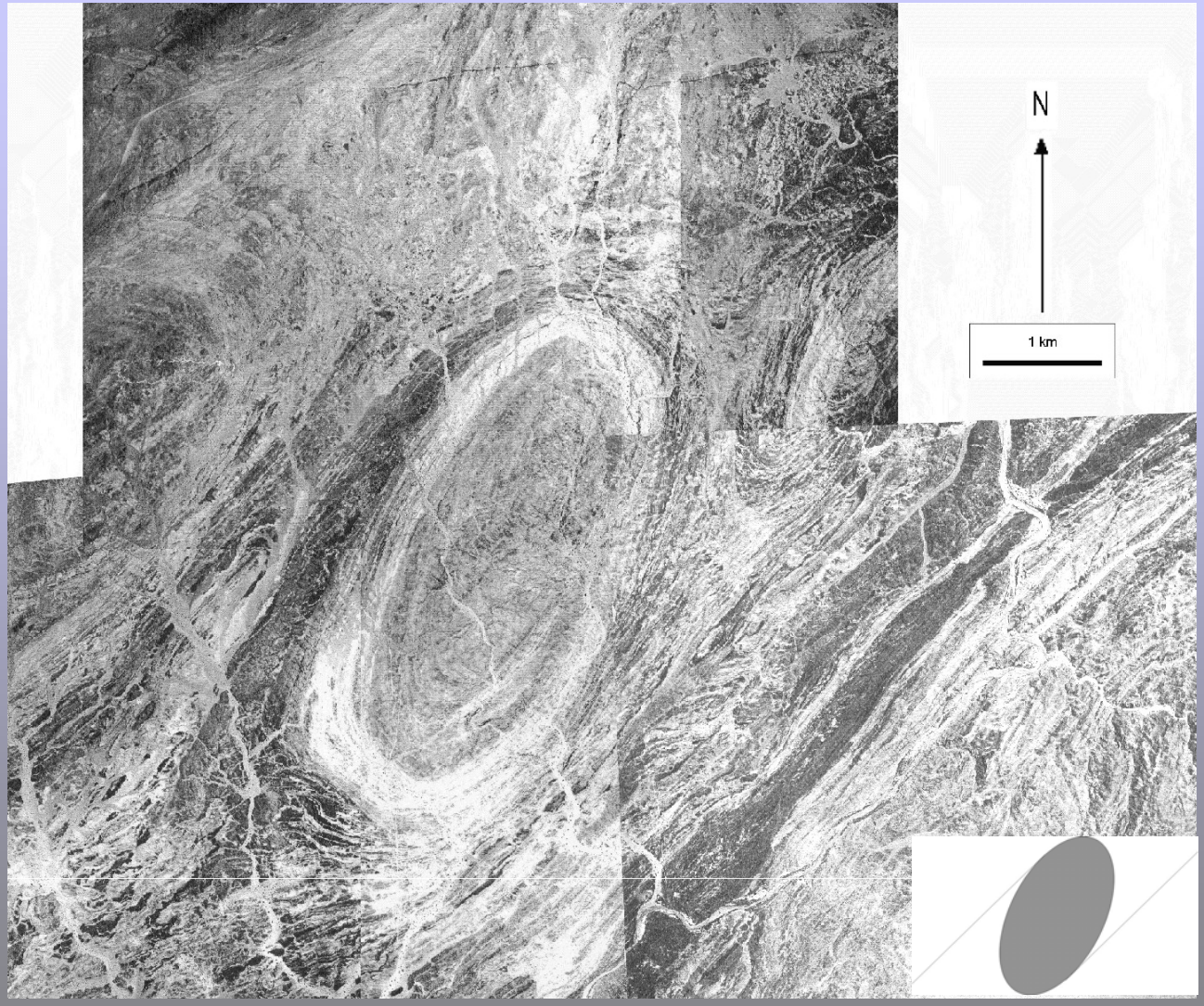

Mosaic of 1:35 000 Scale B+W aerial photographs (Aircraft Operating Company Project 503, Photographs 8870-8876)

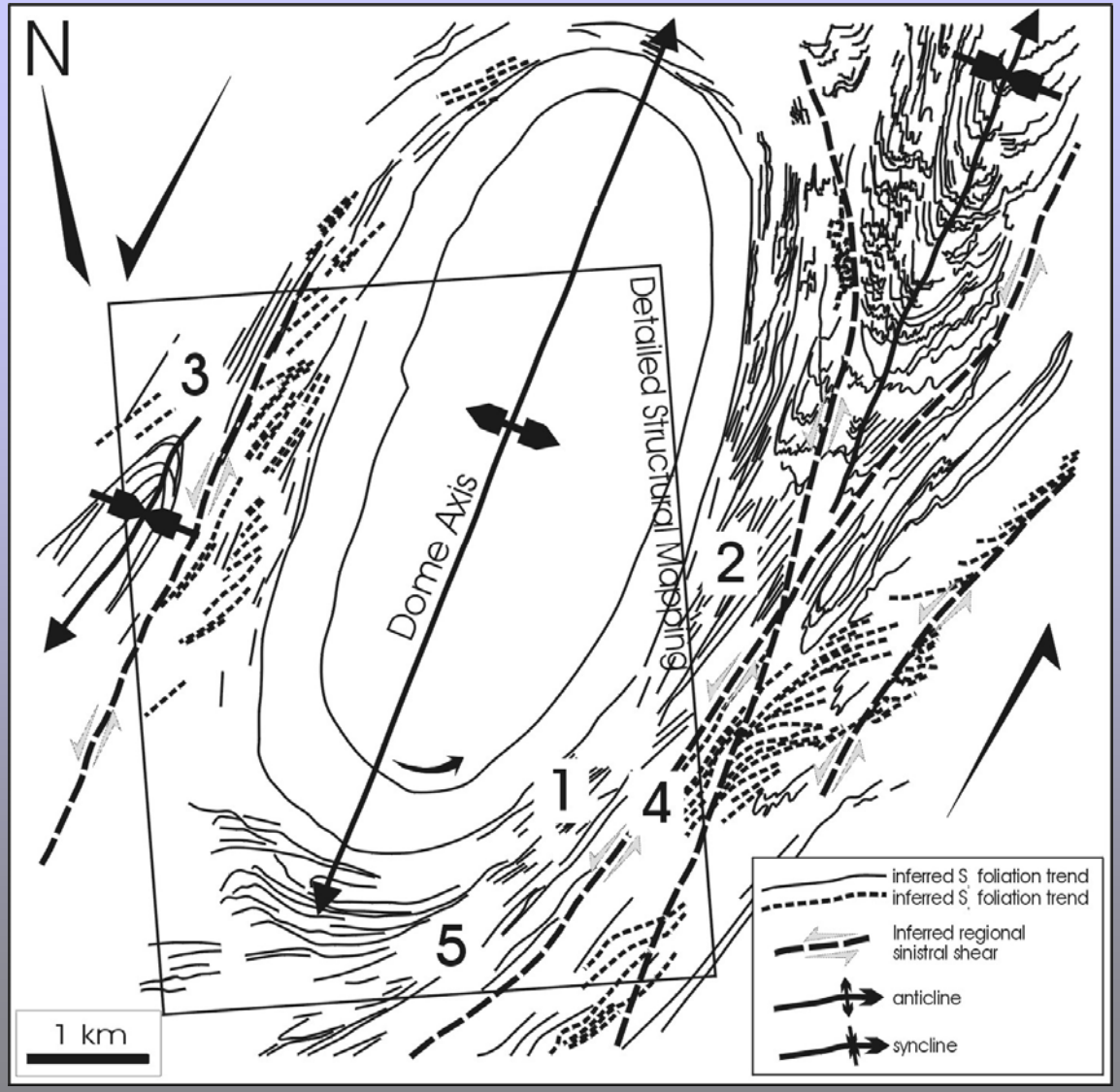

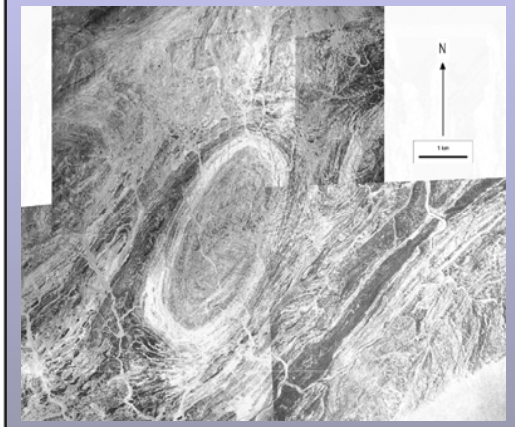

Foliation/Fabric Interpretation of Mosaic of 1:35 000 Scale B+W aerial photographs (Aircraft Operating Company Project 503, Photographs 8870-8876)

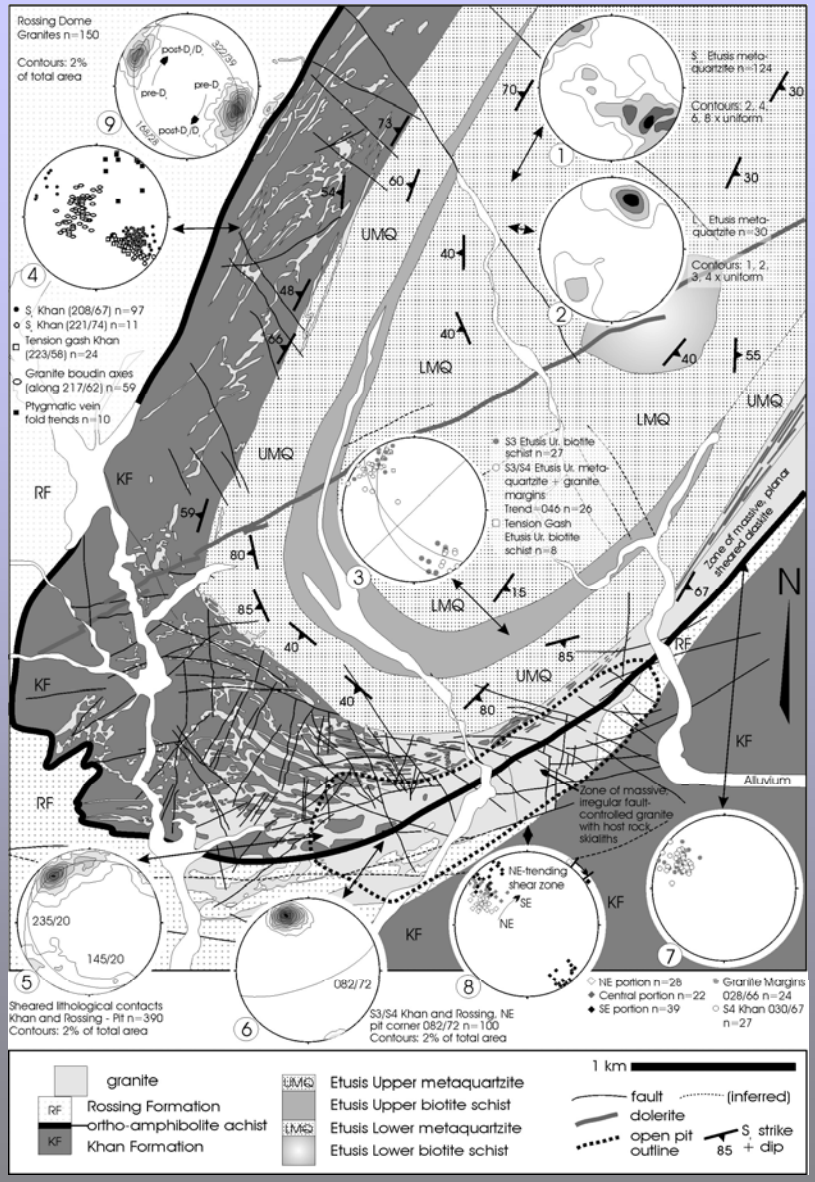

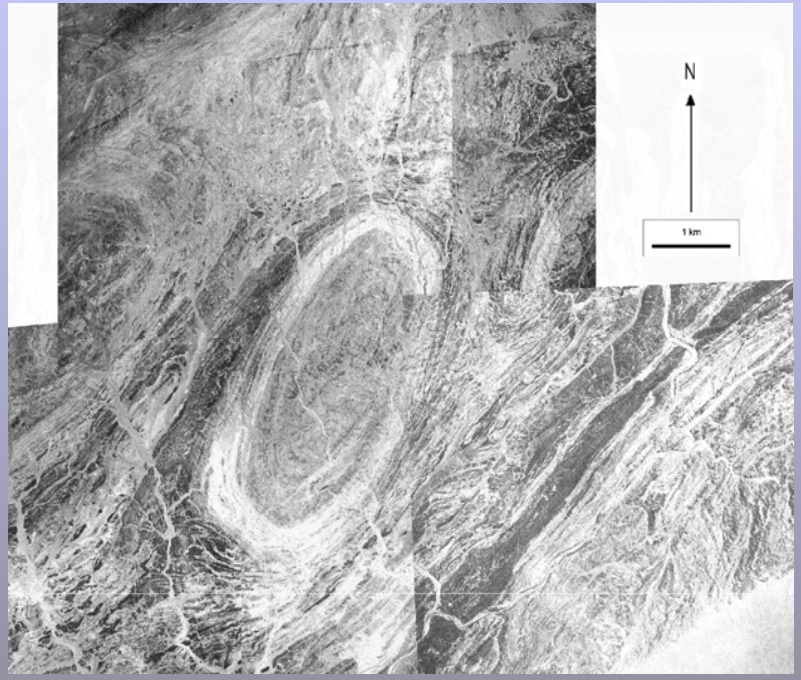

Rössing

Detailed structural map of the southern portion of the Rössing dome, primarily using new data by IJB and dome core data from Oliver and Kinnaird (1996). The pit outline is dotted.

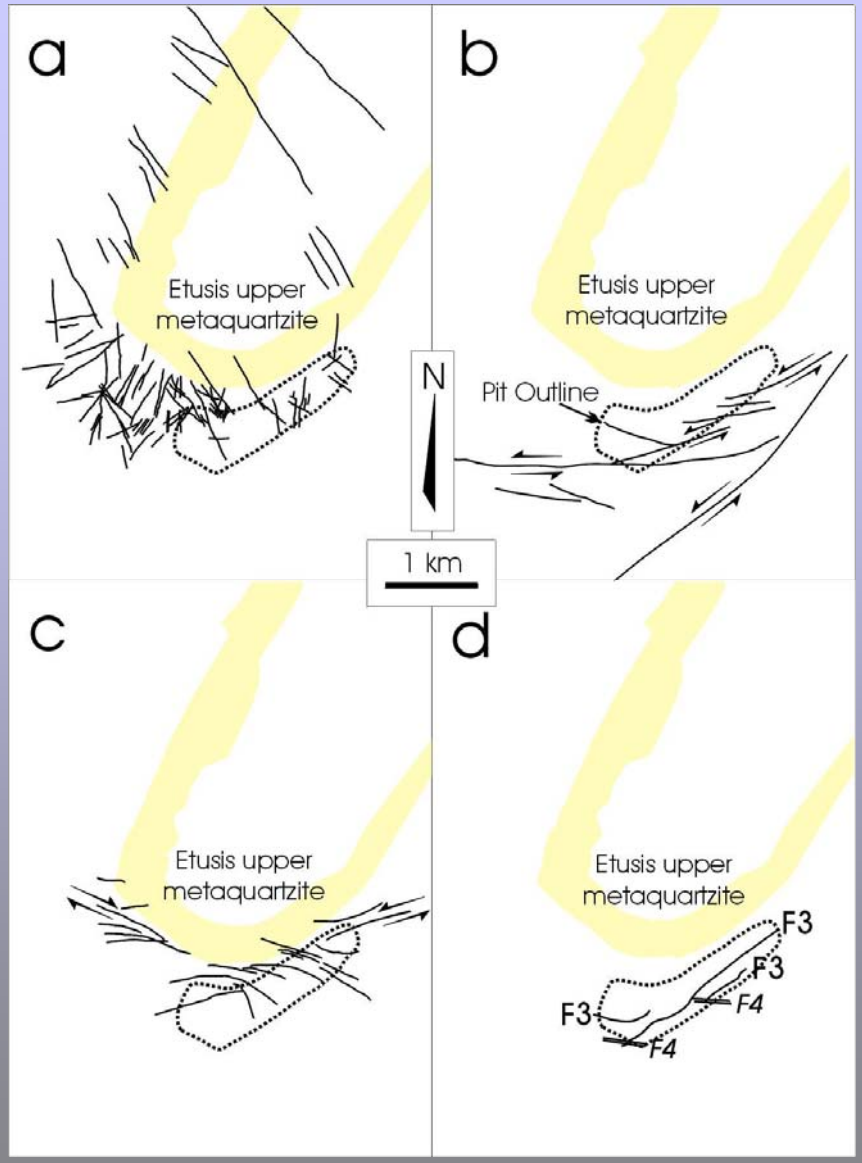

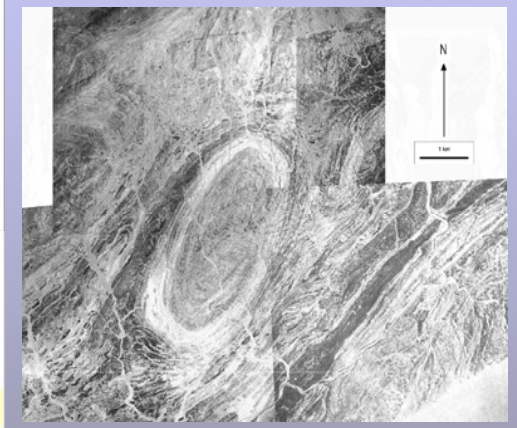

Filtering of unusually abundant interpreted/mapped faults to the south of the competent dome core, according to their nature and offset.

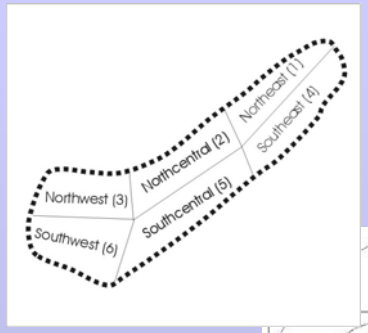

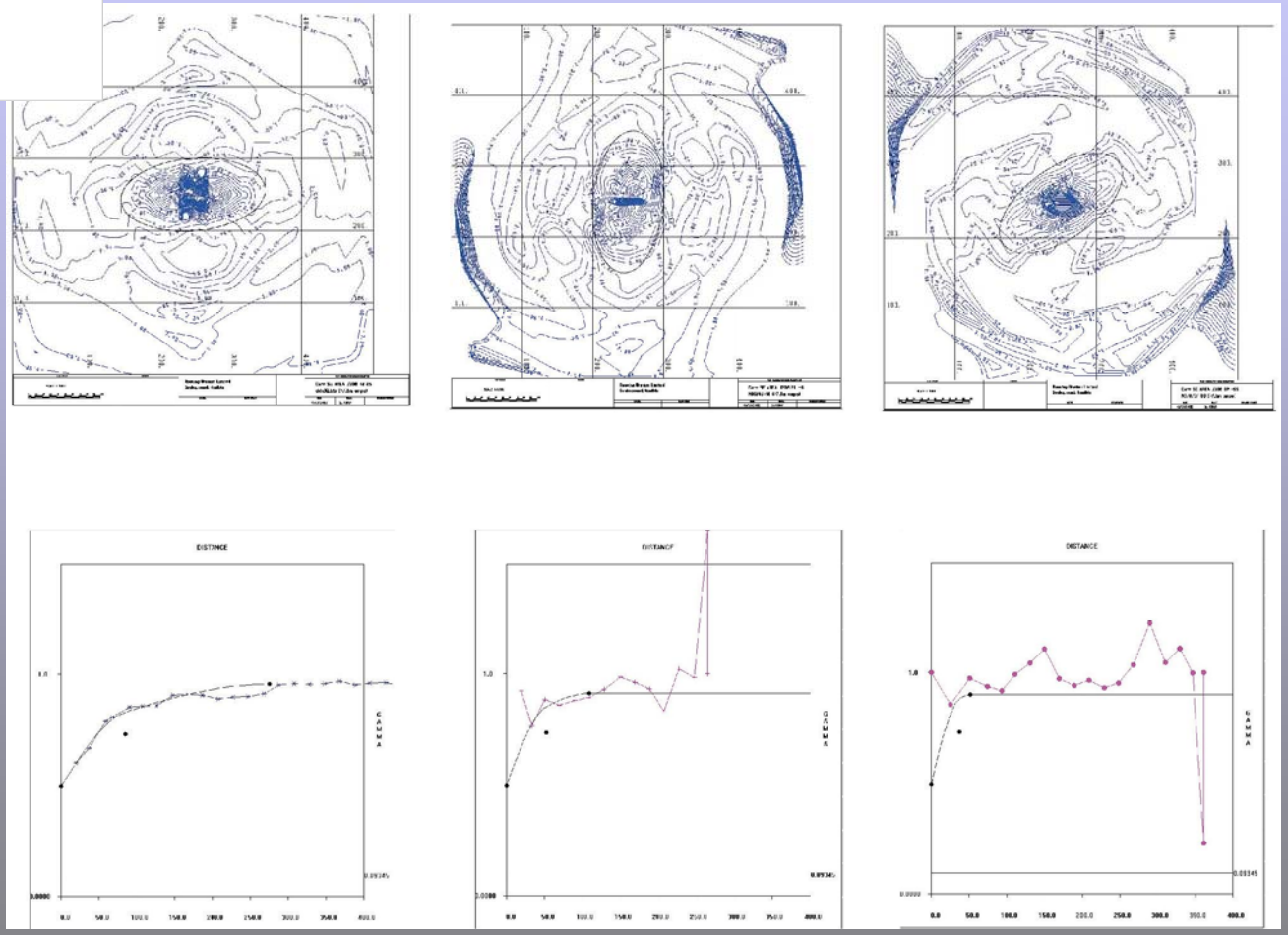

Division of pit into 6 Sectors and an example of 3-Dimensional Semi-Variograms for a given sector. Analysis in Datamine allows for the 3-D morphology and trend of the ore body to be established.

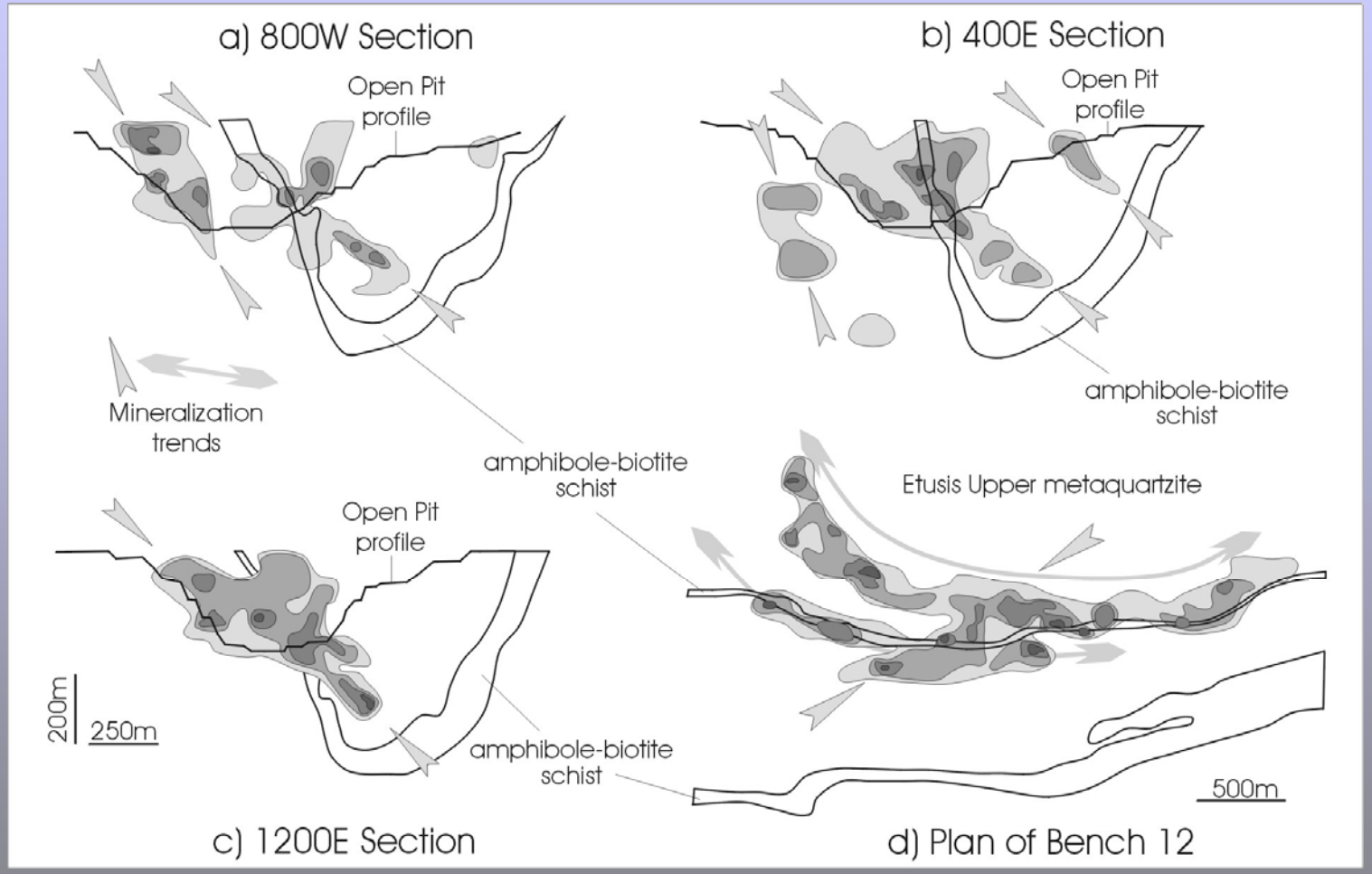

Simplified figures of the distribution of U mineralization. Arrows indicate potentially fault-controlled or dome movement-controlled mineralization trends. Note the discordance between these trends and the amphibole-biotite schist.

Rössing

Lithology/Locality	Dating Method/Mineral	Event Description from Reference	Age (Ma)	Reference	Interpretation (Bowden *et al.*, 1995, 1999; Jacob *et al.*, 2000)	Interpretation (Nex *et al.*, in press, based on Goanikontes area)
Kibaran granitoid-gneiss, Khan River (Abbabis)	U-Pb SHRIMP - zircon cores	Crystallization of basement granite-gneiss	1038±58	Kröner *et al.* (1991)	Minimum age of polycyclic pre-Damara basement	----------
	U-Pb SHRIMP - zircon rims	Damaran metamorphic overprint	571±64	Kröner *et al.* (1991)	*c.* 600-550 Ma – Peak transpressional tectonism and metamorphism – Oblique N-S collision of Kalahari and Congo Cratons (doming?)	Orogenesis, continental collision and crustal thickening Intrusion of **Type A** granites Peak Damaran Metamorphism
Mon Repos diorite, Navachab	U-Pb SHRIMP - zircon	Granite intrusion	563±4 to 546±6	Jacob *et al.* (2000)		
Rotekuppe monzogranite, Navachab	U-Pb SHRIMP - zircon	Granite intrusion	543±5 to 539±6	Jacob *et al.* (2000)		
Granitoids, Ida Dome	U-Pb SHRIMP - zircon	Early post-collisional	*c.* 542-526	Bowden *et al.* (1999)	*c.* 542-526 Ma – Transtensional tectonism and metamorphism (doming?)	Syn-metamorphic red granite intrusion
Foliated Red Granite, Goanikontes	U-Pb single ziron	Syn-metamorphic anatexis	534±7	Briqueu *et al.* (1980)		
Unfoliated white-grey granite, Goanikontes	U-Pb - monazite	Syn-metamorphic anatexis	517±7	Briqueu *et al.* (1980)	*c.* 510 Ma - Peak of granite plutonism	Decompression, D_3 deformation and dome formation, continued red and grey granite intrusion Intrusion of **Types B & C** granites Constrictional deformation in high strain zones Post-decompression isobaric annealing and crystallization
Okongava diorite	U-Pb – zircon evaporation	Early-tectonic	516±6	de Kock & Walraven (1994)		
Salem granite, Goas	U-Pb - zircon	Syn-metamorphic intrusion	512±40	Allsopp *et al.* (1983)		
Khan Formation gneisses Goanikontes	U-Pb - monazite	Syn-metamorphic growth	510±3	Briqueu *et al.* (1980)		
Alkali leucogranite ("alaskite"), Goanikontes	U-Pb - **uraninite**	Intrusion/post-tectonic doming	**508±2**	Briqueu *et al.* (1980)	*This study: reactivation of N-S compression, causing left-lateral movement along NNE-trending shears and southward dome impingement at Rössing* *c.* 505-478 Ma (extended to *c.* 429 Ma?) – late/post-tectonic intrusion, cooling and successive closure of minerals at their respective blocking temperatures	Intrusion of **Type D** granite and main **uranium mineralization**
Alkali leucogranite ("alaskite"), Goanikontes	U-Pb - **monazite**	Intrusion/post-tectonic doming	**509±1**	Briqueu *et al.* (1980)		
Donkerhuk granite, Otjimbingwe	U-Pb - zircon	Intrusion/late-tectonic	505±4	Kukla *et al.* (1991)		Intrusion of **Types E & F** granites
Meta-lamprophyre sill, Navachab	U-Pb - SHRIMP, titanite met. overgrowths	Mineralization/cooling below closure	496±12	Jacob *et al.* (2000)		
Mineralized quartz veins, Navachab	U-Pb - SHRIMP, titanite	Mineralization/cooling below closure	494±8 to 500±10	Jacob *et al.* (2000)		
Diorite, Otjozondjou	$^{40}Ar/^{39}Ar$ - hornblende	Cooling below 500°C	478±4	Hawkesworth *et al.* (1983)		Intrusion of Donkerhoek granites (*q.v.* de Kock and Walraven, 1995 Cooling and localized resetting of Rb-Sr ages
Uranium-enriched alkali leucogranite, Rössing area	Rb-Sr biotite (possibly spurious)	Late- to post-tectonic intrusion	**468±8**	Von Backström & Jacob (1978); Kröner & Hawkesworth (1977), Kröner *et al.* (1978)		
Biotite schist, Khan-Swakop River	K-Ar - biotite	Cooling below 300°C	429±17	Clifford (1967)		

Summary of ages of intrusion-related anatexis, metamorphic and tectonic events of the Central Zone (Rb-Sr whole-rock isochrones and errorchrons and U-Pb concordia intercept ages largely excluded) and the specific timing of sheeted leucogranites with reference to the Goanikontes area (Nex *et al.*, in press) and the interpretation of tectonic events by Bowden *et al.* (1995, 1999) and Jacob *et al.* (2000). The age of 1038±58 Ma (Kröner *et al.*, 1991) for the polycyclic pre-Damara Basement is probably a minimum.

Salient features of the highly variable sheeted granites in the Rössing area

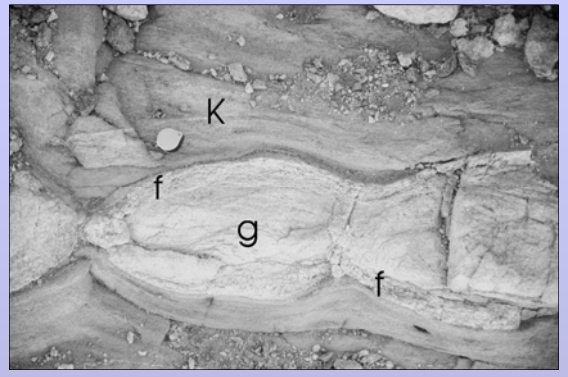

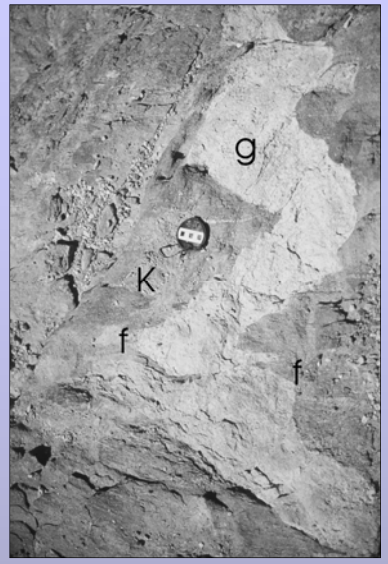

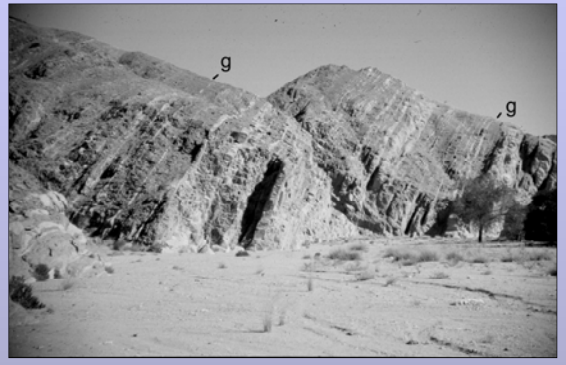

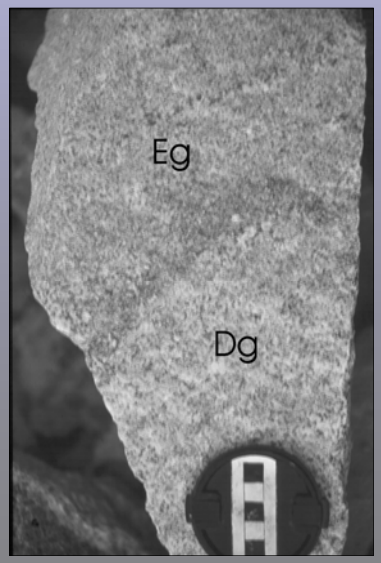

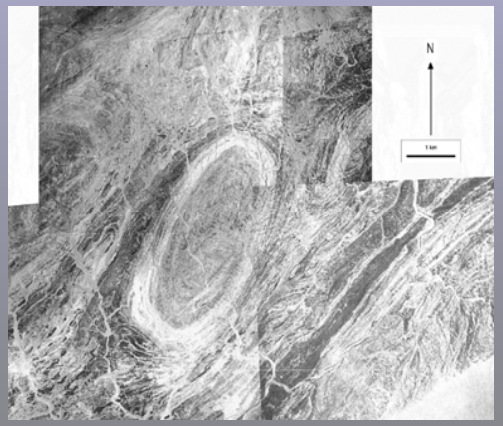

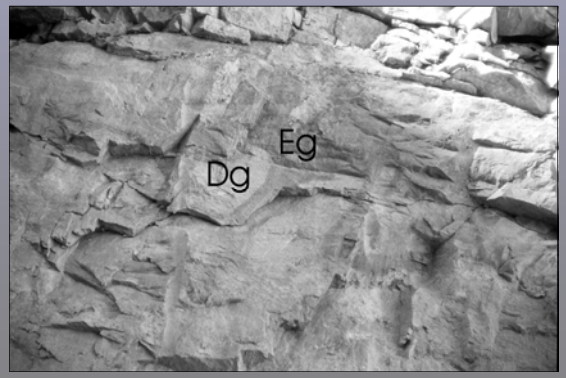

Rössing

Type	Colour	Texture	Mineralogy / Other Features	Goanikontes: Location & Morphology (Nex and Kinnaird, 1995; Nex et al., in press)	Rössing: Key Location Typical Morphology (this study)	Deformation Event (Pre-Post-D_3; Nex et al. in press)
A	Pale pink	Fine- to medium-grained, homogeneous saccharoidal	Dominantly white feldspar	Narrow (<0.75 m) irregular sheets and veins, weakly foliated, boudinaged and folded by D_3, infrequent occurrence	NW dome limb of Khan Formation <0.1 m wide, fine-/medium-grained saccharoidal texture, largely conformable to S_3 foliation; ptygmatic fold axes are parallel to the F_3 axial-planar foliation (Fig. X)	Pre-D_3
B	Dominantly white	Fine-grained to pegmatitic (variable)	Garnetiferous, with tourmaline and biotite as infrequent accessory minerals	Sheets boudinaged and folded by D_3, common outside high strain zone, weakly foliated	NW and SE dome limbs of Khan Formation 0.1 to 2 m wide, often strongly boudinaged with weak imposed S_3 foliation at margins (Fig. X)	Pre-D_3
C	White to pale pink	Medium-grained pegmatitic with clear interstitial quartz	Two feldspar populations, accessory magnetite, ilmenite and tourmaline	Abundant, dominant in relatively undeformed cover sequence, occasionally boudinaged and occurs in F_3 flexures	NW and SE dome limbs of Khan Formation, dome core Etusis Formation 0.1-0.5 m wide, frequently at high angle to foliation and pre-intruded granites, may show plane strain and partial development of weak S_3 foliation (Fig. X)	Pre-D_3
D	White	Medium- to coarse-grained, granular texture more variable than other leucogranite types	Host rock to primary **uranium mineralization**, white feldspar, characteristic smoky quartz, betauranophane occasional betafite and apatite	Extremely irregular; and anastomosing, concentrated in high strain zones along the Khan/Rössing contact (i.e. sheared amphibole –biotite schist)	Dilated S_4 in NW dome limb of Khan Formation, fault network in Rössing Mine, highly attenuated (high strain) Khan Formation "streaming" to the NE from the southern dome core tip 0.2 to 3 m wide, partially replaced by Type E and F granites at mine (Fig. X)	Post-D_3 (509±1 Ma; U-Pb monazite age, Briqueu *et al.*, 1980)?
E	Red to pink, very variable colour with "oxidation haloes"	Extremely variable – fine-grained to very coarse pegmatitic	Similar to Type D or consists almost entirely of smoky/black quartz and pink feldspar	Irregular, tabular to bifurcating bodies in high strain zones, generally emplaced parallel to foliation in basement rocks	Dilated S_4 in NW dome limb of Khan Formation, fault network in Rössing Mine, highly attenuated (high strain) Khan Formation "streaming" to the NE from the southern dome core tip approx. 30 m wide massive tabular bodies (Fig. X)	Post-D_3
F	Red (distinctive)	Coarse-grained pegmatitic	Pink, coarse perthitic feldspar, milky quartz, accessory biotite, magnetite and ilmenite	Tabular bodies with parallel sides, cross-cuts all other structural features	Fault network in Rössing Mine, Dome core - Etusis Formation; massive extensive outcrops to SE of mine approx. 30-40 m wide massive tabular bodies (Fig. X)	Post-D_3

Salient features of granite/leucogranite types recognized in the Swakop River area (Goanikontes), summarized from Nex and Kinnaird (1995) and Nex *et al.* (in press), and the Rössing Area (this study).

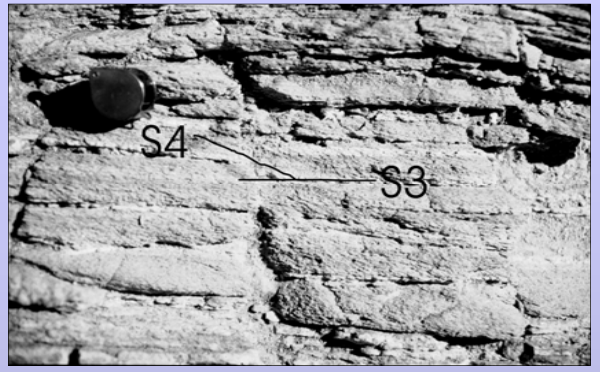

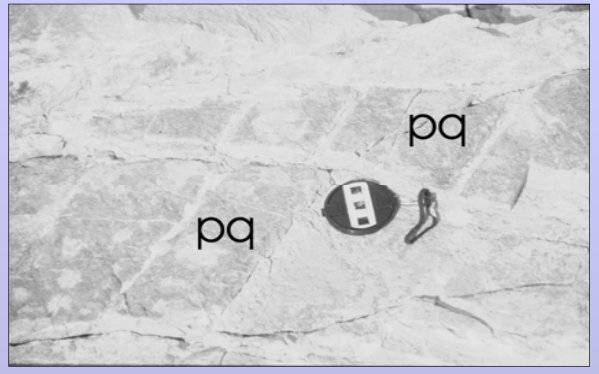

Salient structural features in the Rössing area

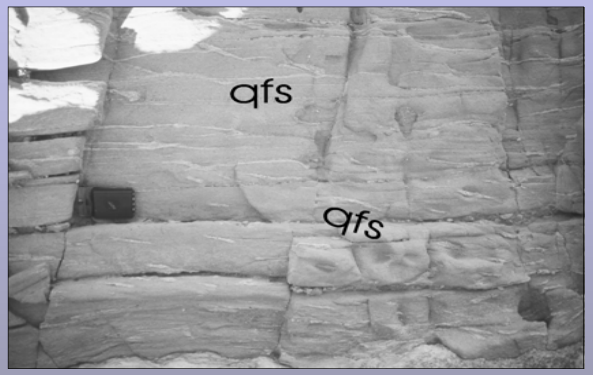

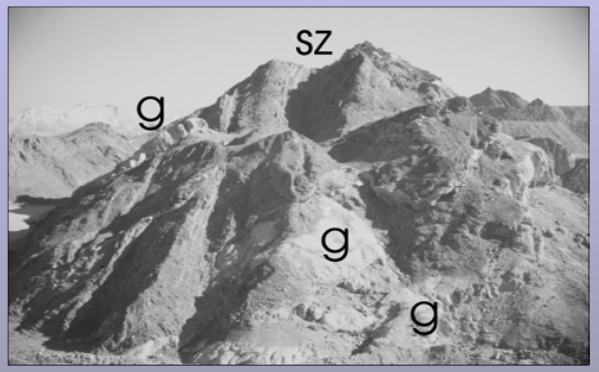

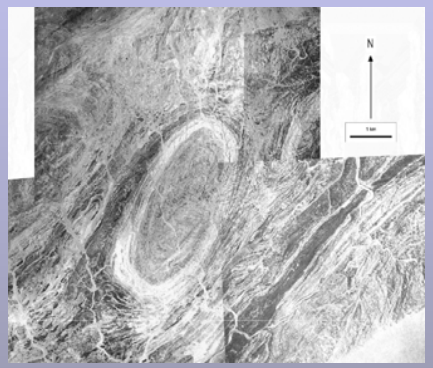

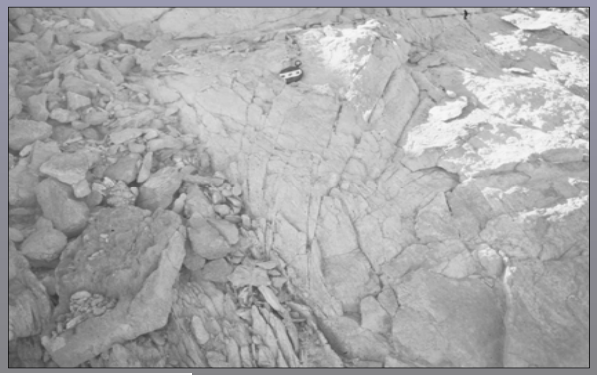

Rössing

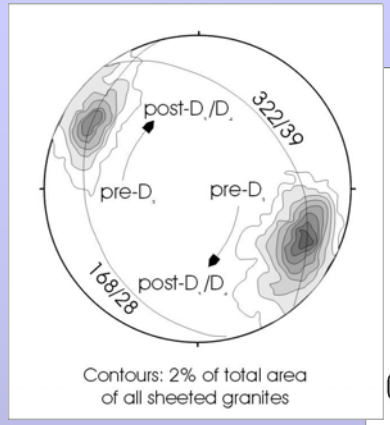

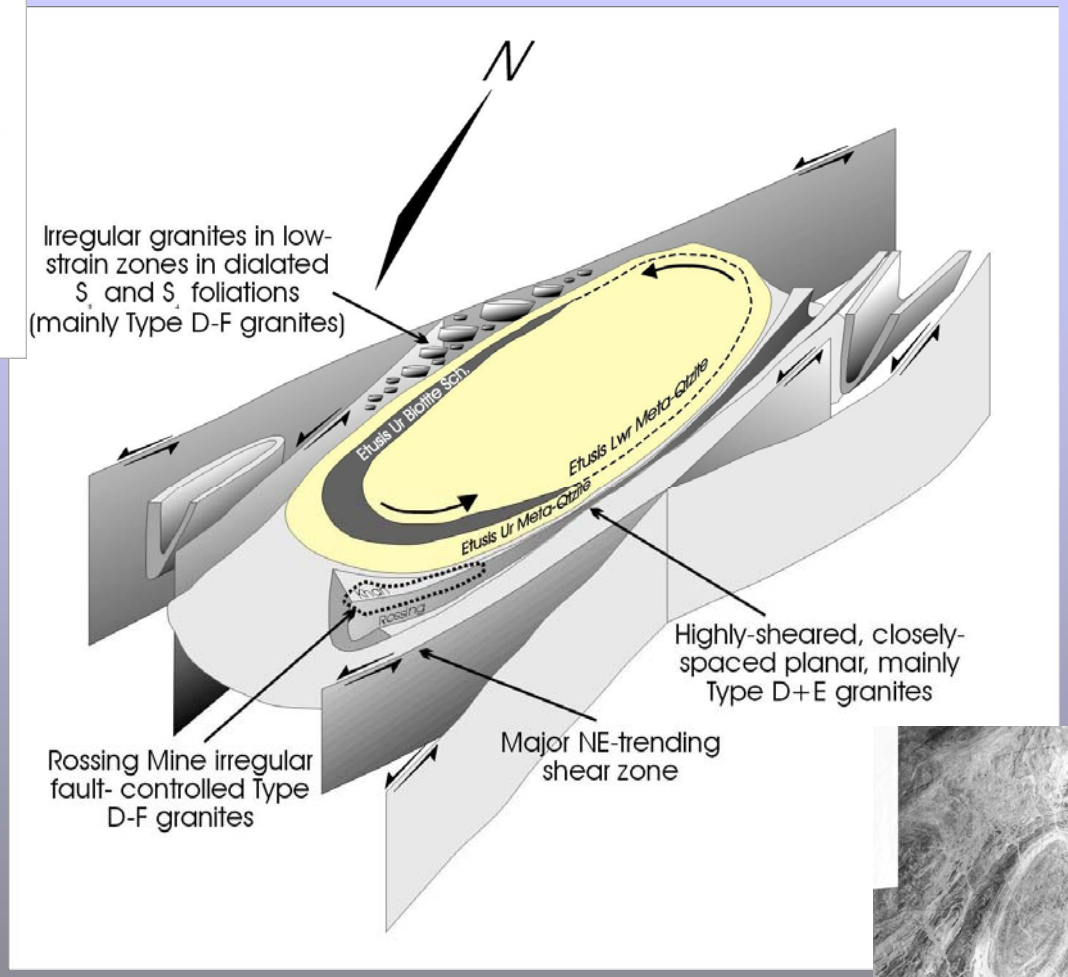

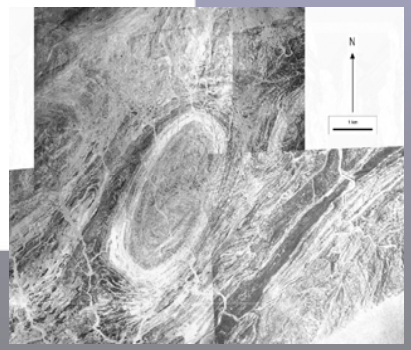

3-D block model of the Rössing Dome, showing the main structural features which indicate anticlockwise late-tectonic/D_4 dome rotation by approximately 27° (inset shows contoured poles to all sheeted granites measured in the Dome).

Rössing

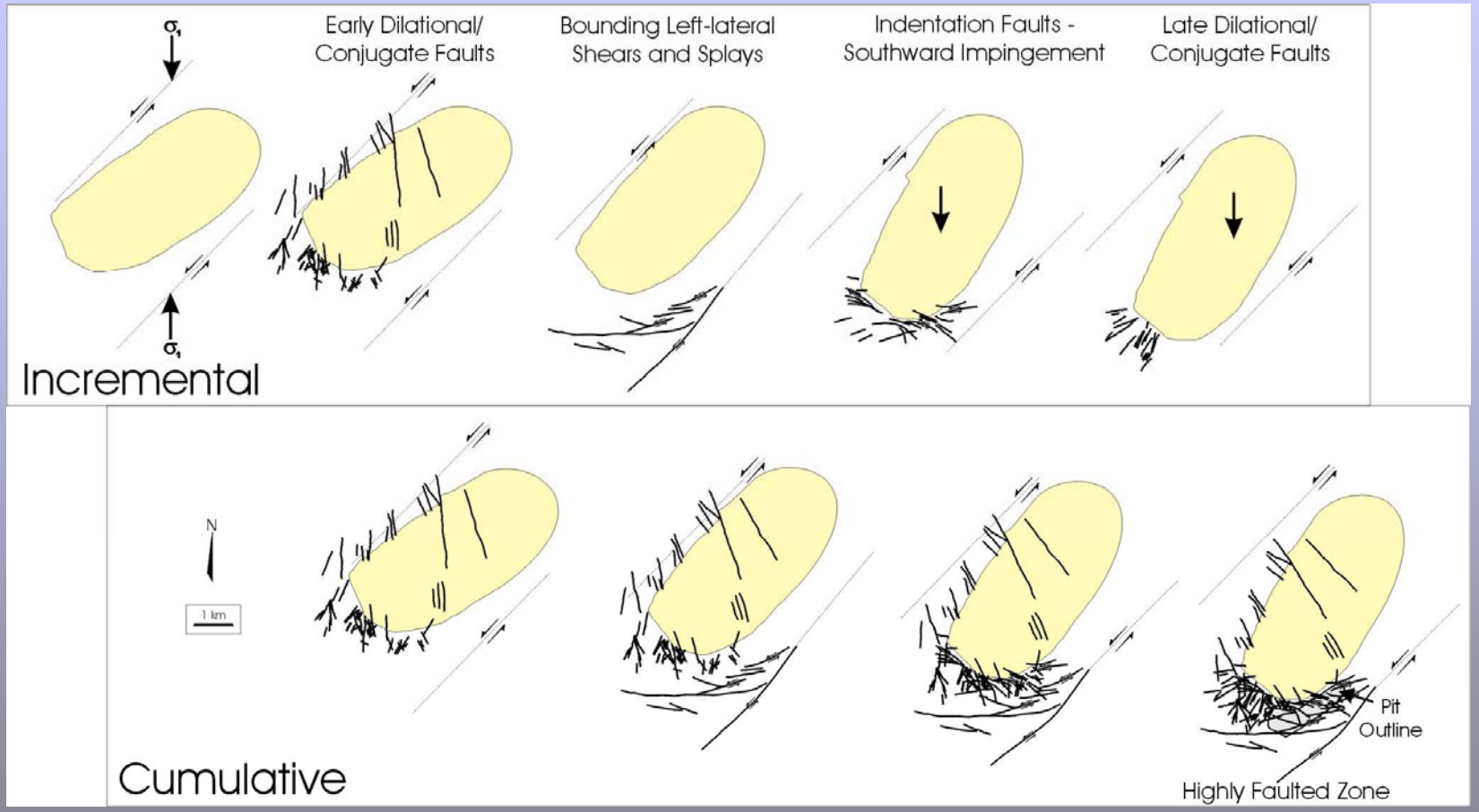

Proposed incremental and cumulative sequence of faulting to the south of the Rössing Dome, which rotated anticlockwise and impinged southwards during the D_4 intrusion of granite types D, E and F. The Rössing ore body occurs in the high-strain portion of an intensely-faulted zone.

Conclusions

- Economically-important alkali-leucogranites ("alaskites") intruded in a post-doming, late-tectonic (D_4) stage of the evolution of the Central Zone of the Damara Orogenic Belt

- Type D (and E) D_4 granites pervasively intruded to the south of the southern tip of the core of the Rössing Dome; granites are proposed to be related to an unusually abundant fault network

- Economic U mineralization within these abundant granites is distributed concentrically around the southern tip of the Etusis Upper Metaquartzite

- The fault network and the enhanced U mineralization were caused by (D_4) southward impingement and anticlockwise rotation of the competent metaquartzite dome core and its interaction with the overlying Khan and Rössing Formations

- Dome movement relates to underlying block movement, in turn related to NNE-trending (Welwitschia Trend) late-tectonic, left-lateral shearing

- Supported by siting of U mineralization to the south of the Ida and Valencia Domes

- Possible further work might include photogeological and structural studies of other domes and microstructural work to confirm large-scale shear-sense indicators

Rössing